
DEEP POLICIES FOR ONLINE BIPARTITE MATCHING: A REINFORCEMENT LEARNING APPROACH

Mohammad Ali Alomrani

Department of Electrical & Computer Engineering
University of Toronto
mohammad.alomrani@mail.utoronto.ca

Reza Moravej

Department of Computer Science
University of Toronto
mreza.moravej@mail.utoronto.ca

Elias B. Khalil

Department of Mechanical & Industrial Engineering
SCALE AI Research Chair in Data-Driven Algorithms for Modern Supply Chains
University of Toronto
khalil@mie.utoronto.ca

ABSTRACT

From assigning computing tasks to servers and advertisements to users, sequential online matching problems arise in a wide variety of domains. The challenge in online matching lies in making irrevocable assignments while there is uncertainty about future inputs. In the theoretical computer science literature, most policies are myopic or greedy in nature. In real-world applications where the matching process is repeated on a regular basis, the underlying data distribution can be leveraged for better decision-making. We present an end-to-end Reinforcement Learning framework for deriving better matching policies based on trial-and-error on historical data. We devise a set of neural network architectures, design feature representations, and empirically evaluate them across two online matching problems: Edge-Weighted Online Bipartite Matching and Online Submodular Bipartite Matching. We show that most of the learning approaches perform significantly better than classical greedy algorithms on four synthetic and real-world datasets. Our code is publicly available at <https://github.com/lyeskhilil/CORL.git>.

1 Introduction

Originally introduced by Karp et al. [21], the Online Bipartite Matching (OBM) problem is a simple formulation of sequential resource allocation. A fixed set U of known entities (e.g., ads, tasks, servers) are to be dynamically assigned to at most one of a discrete stream V of (apriori unknown) entities (e.g., ad-slots, job candidates, computing job) upon their arrival, so as to maximize the size of the final matching. Matching decisions are irrevocable and not matching is allowed at all times. Despite its simplicity, finding better algorithms for OBM and its variants remains an active area of research. The uncertainty about future inputs makes online problems inherently challenging. While practical exact methods (e.g., using integer programming formulations and solvers) exist for many offline combinatorial problems, the restriction to irrevocable and instant decision-making makes impractical the use of such algorithmic tools. Existing algorithms for online matching are thus typically myopic and greedy in nature [26]. In practice, however, the underlying (bipartite) graph instances may come from the same unknown distribution [5]. In many applications, a sufficiently large collection of samples from the data can represent the statistical properties of the entire underlying data-generating distribution. It is often the case that corporations, for example, have access to a wealth of information that is represented as a large graph instance capturing customer behaviour, job arrivals, etc. Thus, it is sensible for an algorithm to use historical data to derive statistical information about online inputs in order to perform better on future instances. However, the use of past data by hand-designed algorithms has been restricted to merely estimating the arrival distribution of the incoming nodes [5, 26]. The downside of this approach is that imperative information such as the graph sparsity, ratio of incoming nodes to fixed nodes, existence of community

structures, degree distribution, and the occurrence of structural motifs are ignored. Ideally, a matching policy should be able to leverage such information to refine its decisions based on the observed history.

In this work, we formulate online matching as a Markov Decision Process (MDP) for which a neural network is trained using Reinforcement Learning (RL) on past graph instances to make near-optimal matchings on unseen test instances. We design six unique models, engineer a set of generic features, and test their performance on two variations of OBM across two synthetic datasets and two real-world datasets. The advantages of our approach can be summarized as follows:

Automating matching policy design: Motivated by practical applications, other variants of OBM have been introduced with additional constraints or more complex objective functions than just matching size. Our method reduces the reliance on human handcrafting of algorithms for each individual variant of OBM since the RL framework presented herein can flexibly model them; this will be demonstrated for the novel Online Submodular Bipartite Matching problem [12].

Deriving tailored policies using past graph instances: We show that our method is capable of taking advantage of past instances to learn a near-optimal policy that is tailored to the problem instance. Unlike "pen-and-paper" algorithms, our use of historical information is not limited to estimating the arrival distribution of incoming nodes. Rather, our method takes advantage of additional statistics such as the existing (partial) matching, graph sparsity, the $|U|$ -to- $|V|$ ratio, and the graph structure. Taking in a more comprehensive set of statistics into account allows for fine-grained decision-making. For example, the RL agent can learn to skip matching a node strategically based on the observed statistical properties of the current graph. Our results on synthetic and real world datasets demonstrate this.

Leveraging Node Attributes: In many variants of OBM, nodes have identities, e.g., the nodes in V could correspond to social media users whose demographic information could be used to understand their preferences. Existing algorithms are limited in considering such node features that could potentially be leveraged to obtain better solutions. For instance, the RL agent may learn that connecting a node v with a particular set of attributes to a specific node in U would yield high returns. The proposed framework can naturally account for such attributes, going beyond simple greedy-like policies. We will show that accounting for node attributes yields improved results on a real-world dataset for Online Submodular Bipartite Matching.

2 Problem Setting

In a bipartite graph $G = (U, V, E)$, U and V are sets of nodes and E is the set of edges connecting a node in U to one in V . In the online bipartite matching problem, the vertex set U is fixed and at each time step a new node $v \in V$ and its edges $\{(u, v) : u \in U\}$ arrive. The algorithm must make an *instantaneous* and *irrevocable* decision to match v to one of its neighbor or not match at all. Nodes in U can be matched to at most one node in V . The time horizon $T = |V|$ is finite and assumed to be known in advance.

The simplest generalization of OBM is the edge-weighted OBM (E-OBM), where a non-negative weight is associated with each edge. Other well-known variants include Adwords, Display Ads and Online Submodular Welfare Maximization [26]. We will focus our experiments on E-OBM and Online Submodular Bipartite Matching (OSBM), a new variation of the problem introduced by Dickerson et al. [12]; together, the two problems span a wide range in problem complexity. The general framework can be extended with little effort to address other online matching problems with different constraints and objectives; see Appendix G for a discussion.

2.1 Edge-weighted OBM (E-OBM)

Each edge $e \in E$ has a predefined weight $w_e \in \mathbb{R}^+$ and the objective is to select a subset S of the incoming edges that maximizes $\sum_{e \in S} w_e$.

2.2 Online Submodular Bipartite Matching (OSBM)

We first define some relevant concepts:

Submodular function: A function $f : 2^U \rightarrow \mathbb{R}^+$, $f(\emptyset) = 0$ is *submodular* iff $\forall S, T \subseteq U$:

$$f(S \cup T) + f(S \cap T) \leq f(S) + f(T).$$

Some common examples of submodular functions include the coverage function, piecewise linear functions, and budget-additive functions. In our experiments, we will focus on the weighted coverage function following [12]:

Coverage function: Given a universe of elements U and a collection of g subsets $A_1, A_2, \dots, A_g \subseteq U$, the function $f(M) = |\cup_{i \in M} A_i|$ is called the coverage function for $M \subseteq \{1, \dots, g\}$. Given a non-negative, monotone weight function $w : 2^U \rightarrow \mathbb{R}^+$, the weighted coverage function is defined analogously as $f(M) = w(\cup_{i \in M} A_i)$ and is known to be submodular.

In this setting, each edge $e \in E$ incident to arriving node v_t has the weight $f(M_t \cup \{e\}) - f(M_t)$ where M_t is the matching at timestep t . The objective in OSBM is to find M such that $f(M) = \sum_{e \in M} w_e$ is maximized; f is a submodular function.

An illustrative application of the OSBM problem, identified by Dickerson et al. [12], can be found in movie recommendation systems. There, the goal is to match incoming users to a set of movies that are both relevant and diverse (genre-wise). A user can login to the platform multiple times and may be recommended (matched to) a movie or left unmatched. Since we have historical information on each user's average ratings for each genre, we can quantify diversity as the weighted coverage function over the set of genres that were matched to the user. The goal is to maximize the sum of the weighted coverage functions for all users. More concretely, if we let U be the universe of genres, then any movie i belongs to a subset of genres A_i . Let L be the set of all users, M_l be the set of movies matched to user l , and $f_l(M_l) = w(\cup_{i \in M_l} A_i)$ be the weighted coverage function defined as the sum of the weights of all genres matched to the user, where the weight of a genre k is the average rating given by user l to movies of genre k . Each user's weighted coverage function is submodular. The objective of OSBM is to maximize the (submodular) sum of these user functions: $f(M) = \sum_{l \in L} f_l(M_l)$.

2.3 Arrival Order

Online problems are studied in different input models that allow the algorithm to access varying amounts of information about the arrival distribution of the vertices in V . The *adversarial* order setting is often used to study the worst-case performance of an algorithm, positing that an imaginary adversary can generate the worst possible graph and input order to make the algorithm perform poorly. More optimistic is the *known i.i.d distribution (KIID)* setting, where the algorithm knows U as well as a distribution \mathcal{D} on the possible *types* of vertices in V . Each arriving vertex v belongs to one type and vertices of a given type have the same neighbours in U . This assumption, i.e., that the arrival distribution \mathcal{D} is given, is too optimistic for noisy real-world applications.

In this work, we study the *unknown i.i.d distribution (UIID)* setting, which lies between the *adversarial* and the *KIID* settings in terms of how much information is given about the arrival distribution [20]. The *unknown i.i.d setting* best captures real-world applications, where a base graph is provided from an existing data set, but an explicit arrival distribution \mathcal{D} is not accessible. For example, a database of past job-to-candidate or item-to-customer relationships can represent a base graph. It is thus safe to assume that the arriving graph will follow the same distribution. More details on data generation in 5.1 and Appendix C.

3 Related Work

Traditional Algorithms for OBM: Generally, the focus of algorithm design for OBM has been on worst-case approximation guarantees for "pen-and-paper" algorithms via competitive analysis, rather than average-case performance in a real-world application. We refer the reader to [20, 26] for a summary of the many results for OBM under various arrival models. On the empirical side, an extensive set of experiments by Borodin et al. [5] showed that the naive greedy algorithm performs similarly to more sophisticated online algorithms on synthetic and real-world graphs in the KIID setting. Though the experiments were limited to OBM with $|U| = |V|$, they were conclusive in that (i) greedy is a strong baseline in practical domains, and (ii) having better proven lower bounds does not necessarily translate into better performance in practice. The main challenge in online problems is decision-making in the face of uncertainty. Many traditional algorithms under the KIID setting aim to overcome this challenge by explicitly approximating the distribution over node types via a type graph. The algorithms observe past instances and estimate the frequency of certain types of online nodes, i.e., for each type i , the algorithm predicts a probability p_i of a node of this type arriving. As noted earlier, the KIID setting is rather simplistic compared to the more realistic UIID setting that we tackle here.

Learning in Combinatorial Optimization: There has recently been substantial progress in using RL for finding better heuristics for offline, NP-complete graph problems. Dai et al. [9] presented an RL-based approach combined with graph embeddings to learn greedy heuristics for some graph problems. Barrett et al. [4] take a similar approach but start with a non-empty solution set and allow the policy to explore by removing nodes/edges from the solution. Chen and Tian [7] learn a secondary policy to pick a particular region of the current solution to modify and incremen-

tally improve the solution. The work by Kool et al. [25] uses an attention based encoder-decoder approach to find high-quality solutions for TSP and other routing problems.

Prior work on using predictive approaches for online problems has been fairly limited. Wang et al. [33] overlook the real-time decision making condition and use Q-learning for a batch of the arriving nodes. The matching process, however, is not done by an RL agent. The work by Kong et al. [24] is one of few to apply RL to online combinatorial optimization. Their work differs from ours in three main ways: (i) the question raised there is whether RL can discover algorithms which perform best on worst-case inputs. They show that the RL agent will eventually learn a policy which follows the "pen-and-paper" algorithm with the best worst-case guarantee. Our work, on the other hand, asks if RL can outperform hand-crafted algorithms on average; (ii) The MDP formulation introduced in [24], unlike ours, does not consider the entire past (nodes that have previously arrived and the existing matching) which can help an RL policy better reason about the future; (iii) our family of invariant neural network architectures apply to graphs of arbitrary sizes $|V|$ and $|U|$. More details about the advantages of our method is provided in the next section.

Online Algorithm Design via Learned Advice: A hybrid paradigm has been recently introduced where the predictive and competitive-analysis approaches are combined to tackle online problems. Such algorithms take advantage of the predictions made by a model to obtain an improved competitive ratio while still guaranteeing a worst-case bound when the predictions are inaccurate. Work in this area has resulted in improvements over traditional algorithms for the secretary, ski rental and online matching problems [3, 32, 10, 28]. Unlike our approach, the model does not get to construct a solution. Rather, its output is used as advice to a secondary algorithm. Since competitive analysis is of concern in this line of work, the algorithm is not treated as a black box and must be explicitly handcrafted for each different online problem. On the other hand, we introduce a general end-to-end framework that can handle online matching problems with different objectives and constraints.

4 Learning Deep Policies for Matching

We now formalize online matching as an MDP, propose a set of models and features, and discuss their properties.

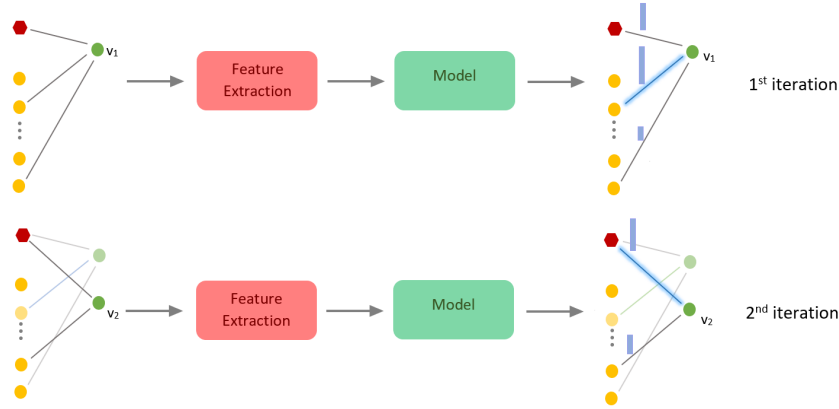


Figure 1: Illustration of how our models match. The red hexagon node represents the “skip” action. At each iteration, the model will take in helpful features about current graph and output a score (the blue bar) for each possible action (an edge or “skip”). This is repeated until all nodes in V have arrived.

4.1 MDP Formulation

The online bipartite matching problem can be formulated in the RL setting as a Markov Decision Process as follows; see Fig. 1 for a high-level illustration:

- **State:** A state S is a set of selected edges (a matching) and the current (partial) bipartite graph G . A terminal state \hat{S} is reached when the final node in V arrives. The length of an episode is $T = |V|$.
- **Action:** The agent has to pick an edge to match or skip. At each timestep t , a node v_t arrives with its edges. The agent can choose to match v_t to one of its neighbors in U or leave it unmatched. Therefore, $|A_t|$, the number of possible actions at time t is $|\text{Nbr}(v)| + 1$, where $\text{Nbr}(v)$ is the set of U nodes with edges to v . Unlike the majority of domains where RL is applied, the uncertainty is exogenous here. Thus, the transition

is *deterministic* regardless of the action picked. That is, the (random) arrival of the next node is independent of the previous actions.

- **Reward function:** The reward $r(s, a)$ is defined as the weight of the edge selected with action a . Hence, the cumulative reward R at the terminal state \hat{S} represents the total weight of the final matching solution:

$$R = \sum_{e \in \hat{S}} w_e$$

- **Policy:** A solution (matching) is a subset of the edges in E , $\pi = \bar{E} \subset E$. A stochastic policy, parameterized by θ , outputs a solution π with probability

$$p_\theta(\pi|G) = \prod_{t=1}^{|V|} p_\theta(\pi_t|s_t),$$

where s_t represents the state at timestep t , G represents the full graph, and π_t represents the action picked at timestep t in solution π .

4.2 Deep Learning Architectures

In this section, we propose a number of architectures that can be utilized to learn effective matching policies. Unless otherwise stated, the models are trained using RL.

Feed-Forward (ff): When node v_t arrives, the ff policy will take as input a vector $(w_0, \dots, w_{|U|}, m_0, \dots, m_{|U|}) \in \mathbb{R}^{2(|U|+1)}$ ¹, where w_u is the weight of the edge from v_t to fixed node u (with $w_u = 0$ if v is not a neighbor of u), and m_u is a binary mask representing the availability of node u for matching. The policy will output a vector of probabilities of size $|U| + 1$, where the additional action represents skipping.

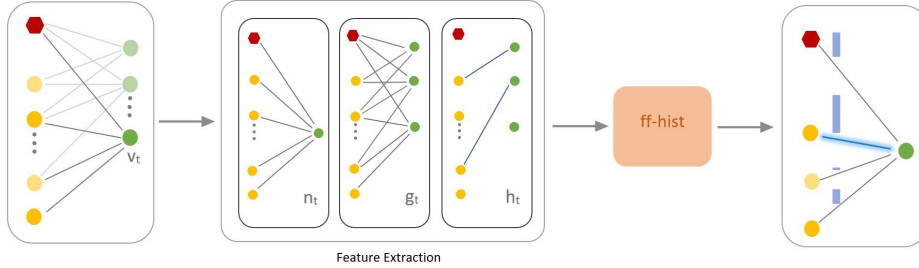


Figure 2: ff-hist Architecture. The model will take in graph-level features for all nodes at once as opposed to invariant models. The graph-level, solution-level and the incoming features are each extracted from the current graph instance and fed into the model which outputs a vector of probabilities. See Table 1 for the detailed list of features.

Feed-Forward with history (ff-hist): This model is similar to ff but takes additional historical information about the current graph to better reason about future input, as shown in Figure 2. That is, ff-hist will take in a vector consisting of five concatenated vectors, (w, m, h_t, g_t, n_t) . The vectors w and m are the same as those in ff. The feature vectors h, n, g contain a range of node-level features such as average weights seen so far per fixed node and solution-level features such as maximum weight in current solution; see Table 1 for details.

Invariant Feed-Forward (inv-ff): We present an invariant architecture, inspired by Andrychowicz et al. [2], which processes each of the edges and their fixed nodes *independently* using the same (shared) feed-forward network. That is, inv-ff will take as input a 3-dimensional vector, (w_u, s_u, w_{mean}) , where w_{mean} is the mean of the edge weights incident to incoming node v_t , and s_u is a binary flag set to 1 if u is the "skip" node. The output for each potential edge is a single number o_u . The vector o is normalized using softmax to output a vector of probabilities, the blue bars in Figure 3.

Invariant Feed-Forward with history (inv-ff-hist): An invariant model, like inv-ff, which utilizes historical information. It is important to note that inv-ff-hist will only look at historical features of one node at a time, in addition to solution-level features. Therefore, the *nodewise* input is $(w_u, m_u, s_u, w_{mean}, n_t, g_{t,u}, h_t)$.

¹The extra input represents the skip node, this not needed for ff and ff-hist, but we add it to make the input consistent across models

Feature type	Description	Equation	Size
Graph-Level Features g_t	Average weight per fixed node u up to time t	$\mu_w = \frac{1}{t} \sum_{\substack{(u,v_i) \in E: \\ v_i \in V, \\ 1 \leq i < t}} w_{(u,v_i)}$	$ U + 1$
	Variance of weights per fixed node u up to time t	$\sigma_w = \frac{1}{t} \sum_{\substack{(u,v_i) \in E: \\ v_i \in V, \\ 1 \leq i < t}} (w_{(u,v_i)} - \mu_w)^2$	$ U + 1$
	Average degree per fixed node u up to time t	$\frac{1}{t} \{(u, v_i) \in E : i \leq t\} $	$ U + 1$
Incoming Node Features n_t	Percentage of fixed nodes incident to incoming v_t (For invariant models only)	$\frac{1}{ U } \{(u, v_t) \in E : u \in U\} $	1
	Normalized step size at time t	$\frac{t}{ V }$	1
Solution-Level Features h_t	Maximum weight in current matching solution	$\max_{e \in S} w_e$	1
	Minimum weight in current matching solution	$\min_{e \in S} w_e$	1
	Mean weight in current matching solution	$\mu_S = \frac{1}{ S } \sum_{e \in S} w_e$	1
	Variance of weights in current matching solution	$\sigma_S = \frac{1}{ S } \sum_{e \in S} (w_e - \mu_S)^2$	1
	Ratio of already matched nodes in U	$\frac{1}{ U } \{(u, v) \in S, u \neq u_{skip}\} $	1
	Ratio of skips made up to time t	$\frac{1}{t} \{(u, v) \in S, u = u_{skip}\} $	1
	The normalized size of current matching solution	$p_t = \frac{1}{ U } \sum_{e \in S} w_e$	1

Table 1: Features used in ff-hist and inv-ff-hist.

Supervised Feed-Forward with history (ff-supervised): To test the advantage of using RL methods, we train ff-hist in a supervised learning fashion. In other words, each incoming node is considered a data sample with a target (the optimal U node to match, in hindsight). During training, after all V nodes have arrived, we minimize the cross-entropy loss across all the samples. This setup is equivalent to behavior cloning [29] where expert demonstrations are divided into state-action pairs and treated as i.i.d samples.

More specifically, for a batch of N bipartite graphs with T incoming nodes, we minimize the weighted cross-entropy loss:

$$\frac{1}{N \times T} \sum_{i=1}^N \sum_{j=1}^T \text{loss}(p_j^i, t_j^i, c)$$

where p_j^i is output of the policy for graph instance i at timestep j , t_j^i is the target, and c is the weight vector of size $|U| + 1$. All classes are given a weight of 1 except the skipping class which is given a weight of $\frac{|U|}{|V|}$. This is to prevent overfitting when most samples belong to the skipping class i.e. when $|V| \gg |U|$ and most incoming nodes are left unmatched. Masking is utilized to prevent all models from picking non-existent edges or already matched nodes.

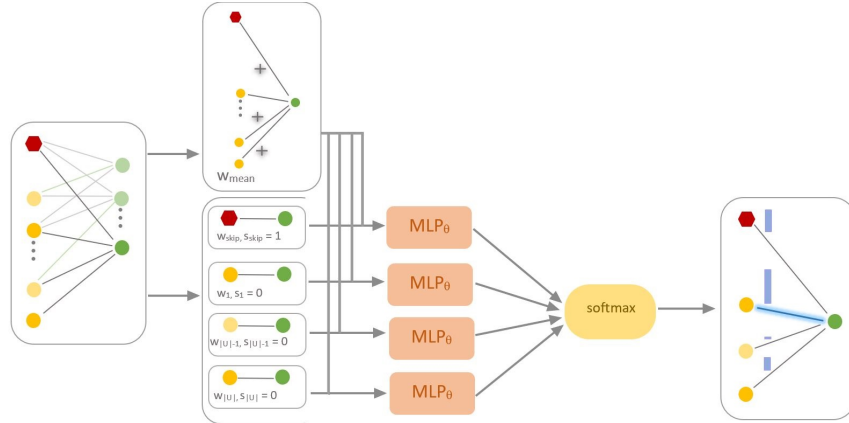


Figure 3: Invariant (inv-ff) Architecture. A shared MLP takes in node specific features and outputs a single number for each node in U . The outputs are then fed into the softmax function to give a vector of probabilities.

Model	Graph size Invariance	Permutation Invariance	History Awareness	Node-feature Awareness	Learnable Parameters
inv-ff	✓	✓			$O((L-1)H^2 + H)$
ff					$O((L-1)H^2 + (U +1)H)$
ff-hist			✓		$O((L-1)H^2 + (U +1)H)$
ff-supervised			✓		$O((L-1)H^2 + (U +1)H)$
inv-ff-hist	✓	✓	✓		$O((L-1)H^2 + H)$
gnn-hist	✓	✓	✓	✓	$O((L-1)H^2 + EH + H + E^2)$

Table 2: Important model characteristics. L: Number of hidden layers, H: Hidden layer size, E: Embedding dimension.

Graph Neural Network (gnn-hist): In this model, we employ the encoder-decoder architecture used in many combinatorial optimization problems, see [6]. At each timestep t , the graph encoder consumes the current graph and produces embeddings for all nodes. The decoder, which also takes *node-wise* inputs, will take in $(w_u, t/T, m_u, s_u, p_t, e_{v_t}, e_u, e_{mean}, e_s)$ where the last four inputs represent the embedding of the incoming node v_t , embedding of the fixed node u being considered, mean embedding of all U nodes, and mean solution embedding, respectively, defined below. Our graph encoder is a MPNN [15] with the weights as edge features. The graph encoder also takes in problem-specific node features if available.

$$e_s = \frac{1}{|S|} \sum_{(u,v) \in S} \Theta_e([e_u; e_v]), \quad (1)$$

$$e_{mean} = \frac{1}{|U|} \sum_{u \in U} e_u. \quad (2)$$

where ";" represents horizontal concatenation and Θ_e is a learnable parameter.

The models outlined above are designed based on a set of desirable properties for matching. Table 2 summarizes the properties that are satisfied by each model:

- **Graph Size Invariance:** Training on large graph instances may be infeasible and costly. Thus, it would be ideal to train a model on small graphs if it generalizes well to larger graphs with a similar generating distribution. We utilize normalization in a way to make sure that each statistic (feature) that we compute lies within a particular range, independent of the graph size. Moreover, the invariant architectures allow us to train small networks that only look at node-wise inputs and share parameters across all fixed nodes. It is also worth noting that the invariance property can be key to OBM variants where U is not fixed, e.g., 2-sided arrivals [11], an application that is left for future work.
- **Permutation Invariance:** In most practical applications, such as assigning jobs to servers or web advertising, the ordering of nodes in the set U should not affect the solution. The invariant architectures ensure that the model outputs the same solution regardless of the permutation of the nodes in U . On the other hand, the non-invariant models such as ff would predict differently for the same graph instance if the U nodes were permuted.
- **History-Awareness:** A state space defined based on the entire current graph and the current matching will allow the model to learn smarter strategies that reason about the future based on the observed past. Historical and graph-based information within the current graph gives the models an "identity" for each fixed node which may be lost due to node-wise input. Contextual features such as n_t and the ratio of already matched nodes help the learned policies to generalize to different graph sizes and U -to- V ratios.
- **Node-feature Awareness:** In real-world scenarios, nodes in U and V represent entities with features that can be key to making good matching decisions. For example, incoming nodes can be users with personal information such as age, gender, and occupation. The node features can be leveraged to obtain better matchings. Our GNN model supports node features. Other models can be modified to take such additional features but would need to be customized to the problem at hand.

4.3 Training Algorithms

Because our focus is on flexible modeling of OBM-type problems with deep learning architectures, we have opted to leverage existing training algorithms with little modification. For RL training, we use the REINFORCE algorithm

Type	Problem	Base Graph Size	Node Attributes?	Weight Generation
ER	E-OBM			$w(u, v) \sim U(0, 1]$
BA	E-OBM			$w(u, v) \sim N(\text{degree}(u), p/5)$
gMission	E-OBM	532 jobs \times 712 workers		payoff for computing the task \times the success probability
MovieLens	OSBM	94 movies \times 200 users	✓	average ratings each user has given for each genre is used as the weights in the coverage function

Table 3: Datasets used for our experiments. More details about datasets and graph instance generation can be found in Appendix C. p is the average node degree in BA graphs.

[30], both for its effectiveness and simplicity, along with a baseline for stabilization. The policy gradient reads:

$$\nabla L(\theta|s) = \mathbb{E}_{p_\theta(\pi|s)}[(L(\pi) - b(s))\nabla \log p_\theta(\pi|s)].$$

To reduce gradient variance and noise, we add a baseline $b(s)$ which is the exponential moving average, $b(s) = M$, where M is the loss $L(\pi)$ in the first training iteration and the update step is $b(s) = \beta M + (1 - \beta)L(\pi)$ [30]. We also utilize entropy regularization to encourage the policies to explore more.

For the supervised training of ff-supervised, we minimize the standard cross-entropy loss as described earlier.

5 Experimental Setup

5.1 Dataset Preparation

We train and test our models across two synthetically generated datasets generated from the Erdos-Renyi (ER) [13] and Barabasi-Albert (BA) [1] graph families. In addition, we use two datasets generated from real-world base graphs. The gMission base graph [8] comes from crowdsourcing data for assigning workers to tasks. We also use MovieLens [18], which is derived from data on users’ ratings of movies based on Dickerson et al. [12].

To generate a bipartite graph instance of size $|U|$ by $|V|$ from the real-world base graph, we sample $|U|$ nodes uniformly at random without replacement from the nodes on the left side of the base graph and sample $|V|$ nodes with replacement from the right side of the base graph. A 10x30 graph is one with $|U| = 10, |V| = 30$, a naming convention we will adopt throughout. More details on the datasets and graph generation can be found in Appendix C.

In our experiments, we generate two versions of each real-world dataset: one where the same fixed nodes are used for all graph instances (gMission, MovieLens), and one where a new set of fixed nodes is generated for each graph instance (gMission-var, MovieLens-var).

5.2 Hyperparameter Tuning and Training Protocol

Full details are deferred to appendices B.3 & B.1. In a nutshell, around 400 configurations, varying four hyperparameters, are explored using Bayesian optimization on a small validation set consisting of small graphs (10x30). We have found the models to be fairly robust to hyperparameter values. In fact, most configurations with low learning rates (under 0.01) result in satisfactory performance as seen in Fig 4. The model with the best (absolute) validation reward is selected for final evaluation, the results of which will be shown in the next section. Some hyperparameters are fixed throughout, particularly the depths/widths of the feed-forward networks (2-3 layers, 100-200 neurons), and the use of the ReLU as activation function. Training often takes less than 6 hours on a NVIDIA v100 GPU.

5.3 Evaluation

Evaluation Metric: We use the *optimality ratio* averaged over the set of test instances. The optimality ratio of a solution S on a graph instance G is defined as $O(S, G) = \frac{c(S)}{OPT(G)}$, where $c(S)$ is the objective value of S and $OPT(G)$ is the optimal value on graph instance G , which is computed in hindsight using integer programming.

Baselines: For E-OBM, we compare our models to the greedy baseline, which simply picks the maximum-weight edge, and greedy-rt [31], a randomized algorithm which is near-optimal in the adversarial setting (see Appendix B.4 for details). For OSBM, we only use greedy as Dickerson et al. [12] find that it achieves better a competitive ratio than their algorithms when movies cannot be matched more than once and the incoming user can be matched to one movie at a time, which is the setting we study here.

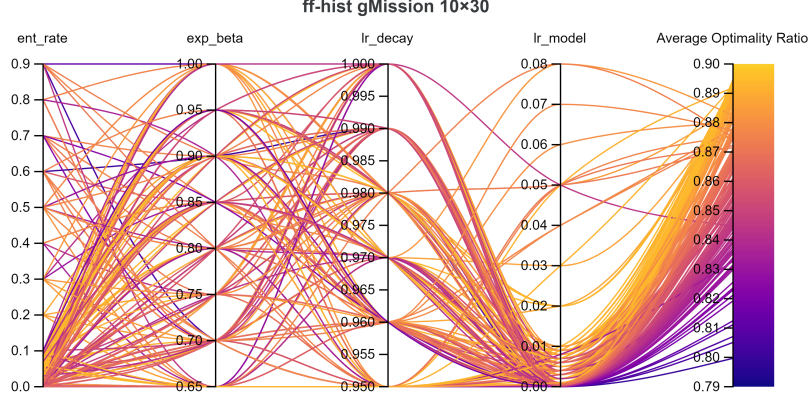


Figure 4: Top 200 hyperparameter tuning results for `ff-hist` on `gMission 10x30`. Each curve represents a hyperparameter configuration. Lighter color means better average optimality ratio on the validation set.

6 Experimental Results

6.1 Edge-Weighted Online Bipartite Matching (E-OBM)

We study the performance of the models across three datasets where the same fixed nodes are used for all graph instances. The edges and weights in the ER graphs are generated from a uniform distribution. ER graphs do not have special graph properties such as the existence of community structures or the occurrence of structural motifs. Thus, the ER dataset is hard to learn from as the models would merely be able to leverage the $|U|$ -to- $|V|$ ratio and the density of the graph (the graph family parameter is proportional to the expected node degree in a graph).

Unlike ER graphs, explicit structural patterns are found in BA graphs. The BA graph generation process is more realistic than ER since it captures more heterogeneous and varied degree distributions which are often witnessed in real world graphs. For example, graphs with many low-degree nodes and a few high-degree nodes occur a lot in practical domains where the rich gets richer phenomenon is witnessed. The BA graph generation process is described in Appendix C. We run the model on BA graphs with average node degree p and degree variance $p/5$ for $p = 5, 15$.

We will also study the models under the `gMission` dataset. Like many real-world datasets, the exact properties of the graphs are unknown. Thus, the models may derive policies based on implicit graph properties. The results demonstrate that the models have taken advantage of some existing patterns in the dataset.

Trends in decisions with respect to the $|U|$ -to- $|V|$ ratio and graph sparsity: The models outperform the two greedy strategies (the two leftmost bars in blue and orange) since they learn that despite missing a short-term reward, skipping would yield a better result in hindsight. As the ER graphs get denser (moving to the right within the first three plots of Fig. 6), the gap between the models and the greedy baselines increases as there is a higher chance of encountering better future options in denser graphs. Hence, the models learn to skip as they find it more rewarding over the long term. This can be further seen in Fig. 5, where the models agree less with greedy on denser ER graphs. For `gMission` (right side of Fig. 5), most disagreements happen in the beginning but all models imitate the optimum towards the end when most actions consist in skipping; Appendix F has more agreement plots.

Outperforming greedy on `100x100` (3rd plot in Fig. 6) ER graphs is quite a difficult task, as there is not much besides the graph density for the models to take advantage of. Since $|V| = |U|$, skipping is also rarely feasible. Hence, the models perform similarly to greedy. Unlike the ER graph, the models are able to leverage properties besides sparsity in `gMission 100x100`, outperforming the greedy baselines (in Fig. 8).

Model-specific Results: Models with history, namely `inv-ff-hist` (pink) and `ff-hist` (purple), consistently outperform their history-less counterparts, `ff` and `inv-ff` across all three datasets (Figures 6, 7, 8).

`inv-ff` receives the same information as greedy and performs fairly similar to it on `gMission` and ER graphs. In fact, `inv-ff` learns to be exactly greedy on `gMission 100x100` (see Appendix F). However, `inv-ff` performs better than other non-invariant models on the BA dataset. The ideal policy on BA graphs would discover that matching to a high-degree node is not wise since the node will likely receive a lot more edges in the future. Similarly, matching to a low-degree node is desired since the node will probably not have many edges in the future. The node-wise reasoning of the invariant models is effective at learning to utilize such node-specific graph property and following

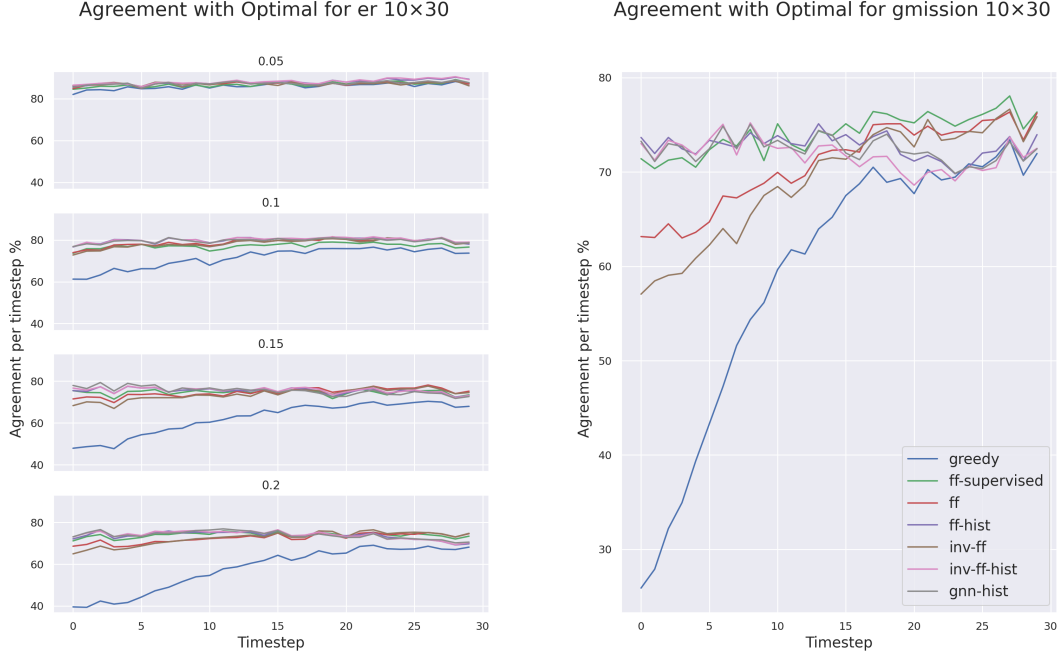


Figure 5: Percent agreement with the optimal solution per timestep. A point (timestep t , agreement a) on this plot can be read as: at timestep t , this method makes the same matching decision as the optimal solution on $a\%$ of the test instances.

a more feasible policy. Armed with historical context, `inv-ff-hist` outperforms all other models on BA graphs (Fig. 7).

The best performance on ER and gMission is achieved by `ff-hist` since the model gets all information (weights) at once (Fig. 8). However, when U nodes are permuted, `inv-ff-hist` vastly outperforms `ff-hist`, as shown in Appendix E.

`ff-supervised` performs well but not as good as RL models since supervised learning comes with its own disadvantages i.e., overfitting when there are more skip actions than match, and being unable to reason sequentially when it makes a wrong decision early on.

Do models trained on small graphs transfer to larger graphs? In Fig. 9, we train all models on 10×30 and 10×60 graphs separately and test their transferability to graphs with different $|U|$ -to- $|V|$ ratios up to size 100×200 . `gnn-hist` and `inv-ff-hist` perform especially well on graphs with similar $|U|$ -to- $|V|$ ratio. For 100×100 graphs, `inv-ff` performs poorly as it does not receive any features that give it context within a new graph size such as number of available fixed nodes.

Some advantages to using invariant models: We also experiment with a variation of the gMission dataset, where a new set of fixed nodes is generated for each graph instance. In Figure 10, we see the same pattern as in gMission (where the same fixed nodes in $|U|$ existed across all instances), except non-invariant models degrade substantially for 100×100 , this is because the input size increased by a lot but the model’s hidden layers’ size were kept constant. A significant disadvantage of non-invariant models is that they are not independent of $|U|$, hence, model size needs to be increased as $|U|$ increases. Invariant models are unaffected by this issue as they reason *node-wise*. We notice that this problem is not seen in gMission. One explanation for this is that fixed nodes are the same across all instances so models have a good idea of the weight distribution for each fixed node which is the same during testing and training. Therefore, even though the model size is not scaled as the input size increases, the models can in some sense "guess" the incoming weights and so do not need as much of an increase in capacity as the number of fixed nodes increases.

Once again, models with history display better performance as history helps the models build a better "identity" of each fixed node as more nodes come in even if never seen during training.

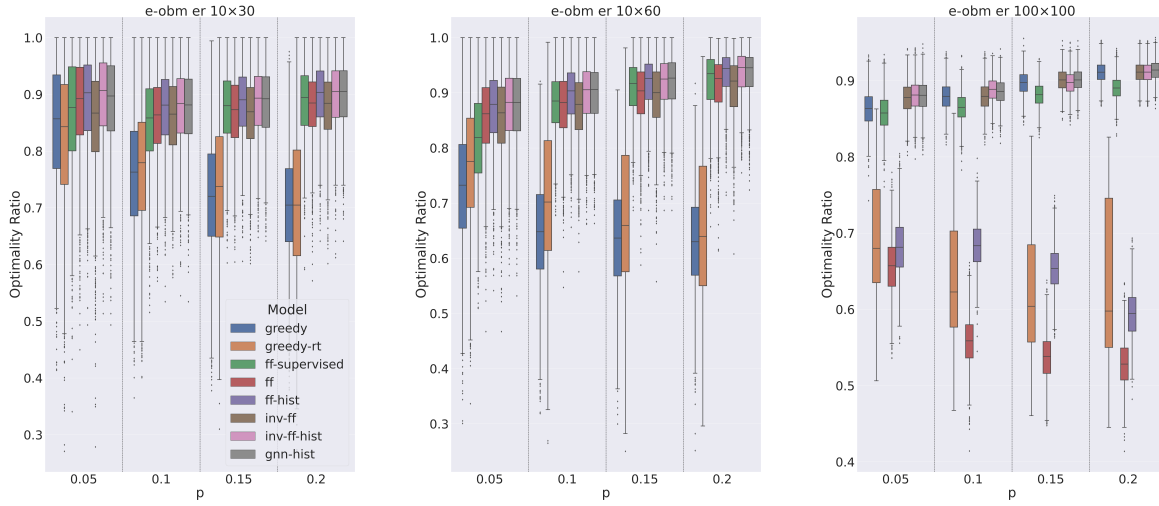


Figure 6: Distributions of the Optimality Ratios for E-OBM on ER graphs. The graph family parameter p is the probability of a random edge existing in the graph.

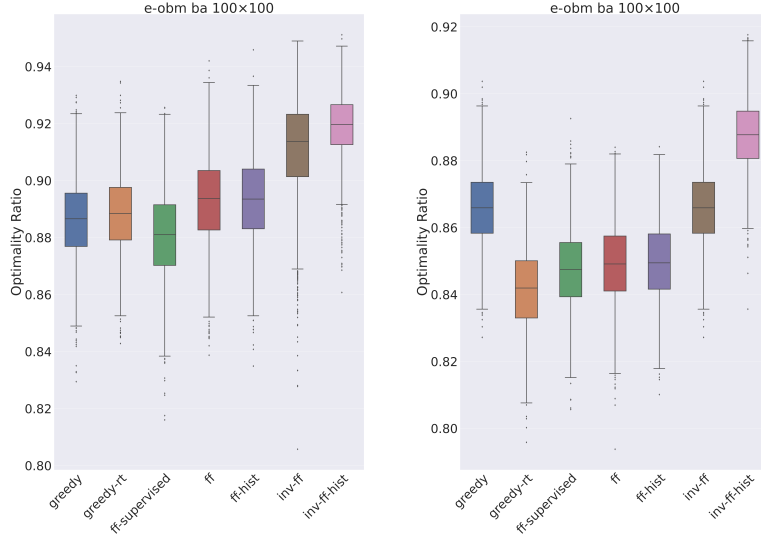


Figure 7: Distributions of the Optimality Ratios for E-OBM on BA graphs with average node degree 5, $w_u \sim N(5, 1)$ (left); BA with average node degree 15, $w_u \sim N(15, 3)$ (right).

6.2 Online Submodular Bipartite Matching (OSBM)

The inherent complexity of the problem as well as the dataset provides the model with more information to leverage. As such, the models tend to discover policies which do significantly better than greedy as shown in Fig. 11. The benefit of RL models is apparent here when compared to ff-supervised, particularly for 10x30 and 94x100 graphs. The relative complexity of OSBM compared to E-OBM will require the model to be more generalizable as the reasoning involved is more complex and mere imitation is not enough. ff-supervised also underperforms because the edge weights depend on the current solution and can change on the same graph instance if previous matches are different, causing a great mismatch with the training data. A similar trend to E-OBM results is observed here: models with history outperform their history-less counterparts. The context provided by history is particularly helpful as

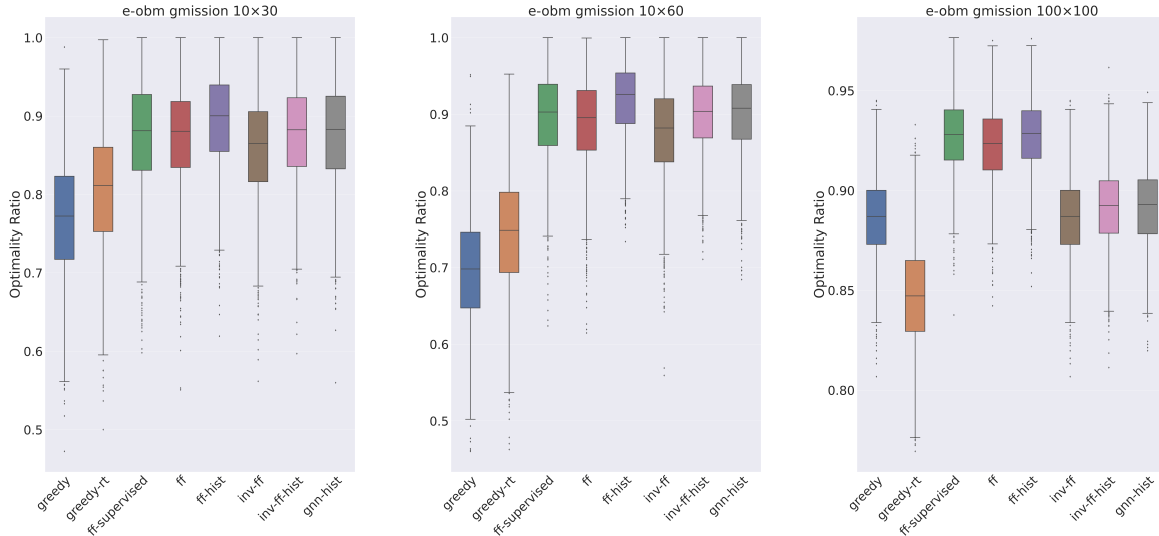


Figure 8: Distributions of the Optimality Ratios for E-OBM on the gMission dataset. Higher is better.

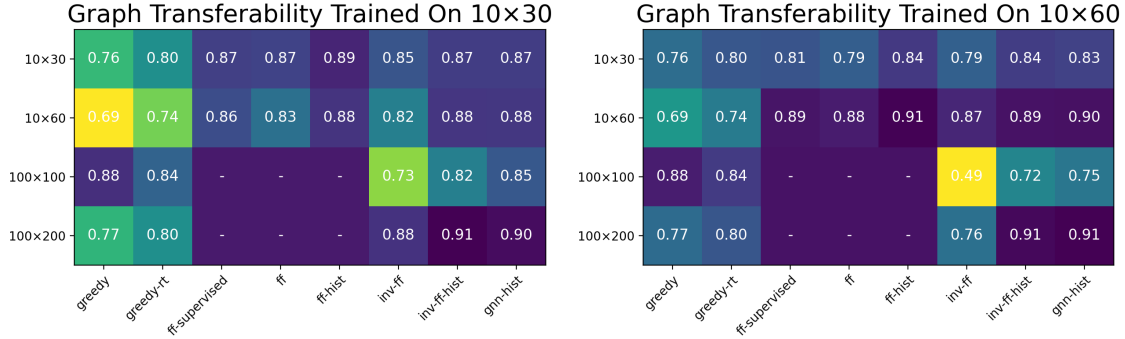


Figure 9: Graph Transferability: Average optimality ratios for models trained on graphs of size 10x30 (left) & 10x60 (right) and tested on graphs of different sizes. Higher (darker) is better. Missing values are denoted with a dash for models that are not invariant to the number of U nodes of the training graphs.

the edge weights depend on previous matches. Furthermore, we notice that **gnn-hist** has the best performance on 10x30 and 94x100 graphs as **gnn-hist** is the only model that uses user attributes as node features.

In Figure 12, we witness the same issue seen in gMission-var results of Figure 10. The non-invariant models degrade on 94x100 graphs due to having the same number of hidden layer despite processing larger graphs. The invariant models remain unaffected by the graph size. Interestingly, the invariant models even slightly outperform their non-invariant counterparts on 10x30 and 10x60 MovieLens-var.

7 Conclusion

Through extensive experiments, we have demonstrated that deep reinforcement learning with appropriately designed neural network architectures and feature engineering can produce high-performance online matching policies across two problems spanning a wide range of complexity. In particular, we make the following concluding observations:

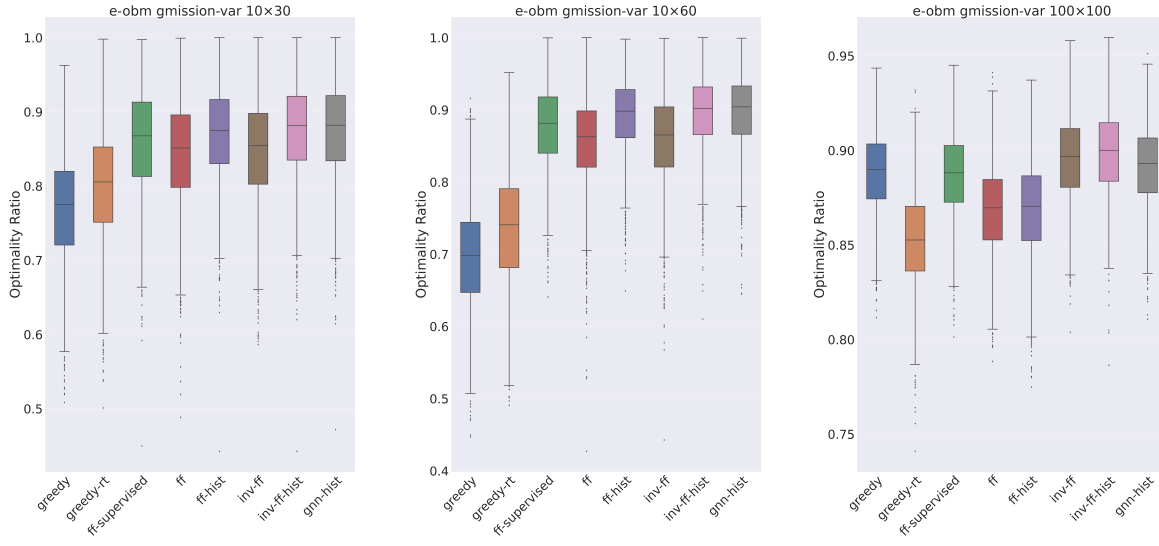


Figure 10: Distributions of the Optimality Ratios for E-OBM on three graph sizes for gMission-var.

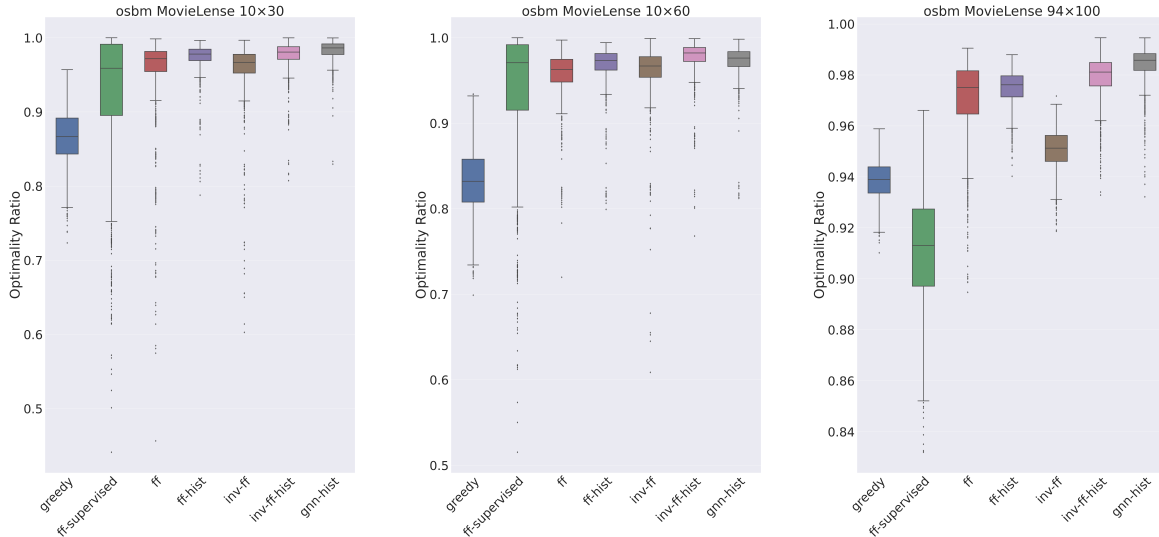


Figure 11: Distributions of the Optimality Ratios for OSBM on three graph sizes for MovieLens. Higher is better.

- A basic reinforcement learning formulation and training scheme are sufficient to produce good learned policies for online matching, are typically not sensitive to the choice of hyperparameters, and are advantageous compared to a supervised learning approach;
- Compared to greedy policies, RL-based policies are more effective, a result that can be partially explained by a stronger agreement with the optimal solution (in hindsight) in the early timesteps of the process when greedy is too eager to match;
- Models that are invariant to the number of nodes are more advantageous than fully-connected models in terms of how well they generalize to test instances that are slightly perturbed compared to the training instances, either in graph size or in the identities of the fixed nodes;

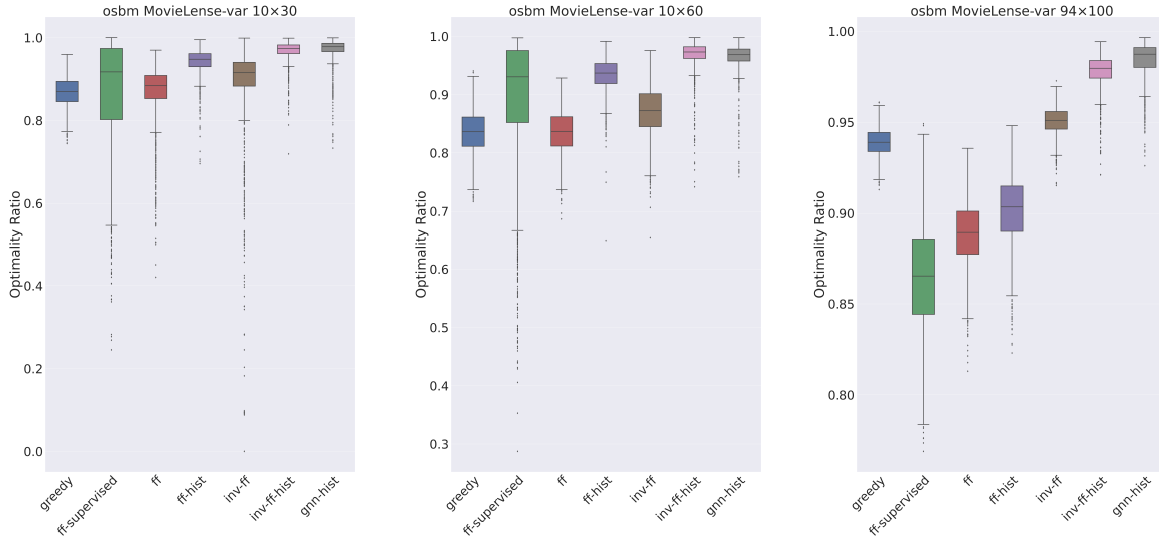


Figure 12: Distributions of the Optimality Ratios for OSBM on three graph sizes for MovieLens-var.

- Feature engineering at the node and graph levels can help model the history of the matching process up to that timestep, resulting in improved solutions compared to models that use only weight information from the current timestep;
- Graph Neural Network models are a viable alternative to feed-forward models as they can leverage node features and their dependencies across nodes more naturally.

Future avenues of research include:

- A more extensive experimental analysis of different RL training algorithms beyond basic policy gradient;
- A proper imitation learning approach that can leverage both the optimal solution in hindsight and the adaptive training common in RL;
- Extensions to new real-world datasets with rich node and edge features that could benefit even more from highly expressive models such as GNNs;
- Extensions to other online combinatorial optimization problems, which can leverage our framework, models, and code as a starting point.

References

- [1] Réka Albert and Albert-László Barabási. Statistical mechanics of complex networks. *Rev. Mod. Phys.*, 74:47–97, Jan 2002. doi:10.1103/RevModPhys.74.47. URL <https://link.aps.org/doi/10.1103/RevModPhys.74.47>.
- [2] Marcin Andrychowicz, Misha Denil, Sergio Gomez, Matthew W Hoffman, David Pfau, Tom Schaul, Brendan Shillingford, and Nando De Freitas. Learning to learn by gradient descent by gradient descent. In *Advances in neural information processing systems*, pages 3981–3989, 2016.
- [3] Antonios Antoniadis, Themis Gouleakis, Pieter Kleer, and Pavel Kolev. Secretary and online matching problems with machine learned advice. In H. Larochelle, M. Ranzato, R. Hadsell, M. F. Balcan, and H. Lin, editors, *Advances in Neural Information Processing Systems*, volume 33, pages 7933–7944. Curran Associates, Inc., 2020. URL <https://proceedings.neurips.cc/paper/2020/file/5a378f8490c8d6af8647a753812f6e31-Paper.pdf>.
- [4] Thomas D. Barrett, William R. Clements, Jakob N. Foerster, and A. I. Lvovsky. Exploratory combinatorial optimization with reinforcement learning. In *The Thirty-Fourth AAAI Conference on Artificial Intelligence, AAAI 2020, The Thirty-Second Innovative Applications of Artificial Intelligence Conference, IAAI 2020, The Tenth AAAI Symposium on Educational Advances in Artificial Intelligence, EAAI 2020, New York, NY, USA, February 7-12, 2020*, pages 3243–3250. AAAI Press, 2020. URL <https://aaai.org/ojs/index.php/AAAI/article/view/5723>.
- [5] Allan Borodin, Christodoulos Karavasilis, and Denis Pankratov. An experimental study of algorithms for online bipartite matching. *ACM J. Exp. Algorithmics*, 25, March 2020. ISSN 1084-6654. doi:10.1145/3379552. URL <https://doi.org/10.1145/3379552>.
- [6] Quentin Cappart, Didier Chételat, Elias B. Khalil, Andrea Lodi, Christopher Morris, and Petar Velickovic. Combinatorial optimization and reasoning with graph neural networks. *CoRR*, abs/2102.09544, 2021. URL <https://arxiv.org/abs/2102.09544>.
- [7] Xinyun Chen and Yuandong Tian. Learning to perform local rewriting for combinatorial optimization. In Hanna M. Wallach, Hugo Larochelle, Alina Beygelzimer, Florence d’Alché-Buc, Emily B. Fox, and Roman Garnett, editors, *Advances in Neural Information Processing Systems 32: Annual Conference on Neural Information Processing Systems 2019, NeurIPS 2019, December 8-14, 2019, Vancouver, BC, Canada*, pages 6278–6289, 2019. URL <https://proceedings.neurips.cc/paper/2019/hash/131f383b434fdf48079bfff1e44e2d9a5-Abstract.html>.
- [8] Zhao Chen, Rui Fu, Ziyuan Zhao, Zheng Liu, Leihao Xia, Lei Chen, Peng Cheng, Caleb Chen Cao, Yongxin Tong, and Chen Jason Zhang. Gmission: A general spatial crowdsourcing platform. *Proc. VLDB Endow.*, 7(13): 1629–1632, August 2014. ISSN 2150-8097. doi:10.14778/2733004.2733047. URL <https://doi.org/10.14778/2733004.2733047>.
- [9] Hanjun Dai, Elias B. Khalil, Yuyu Zhang, Bistra Dilkina, and Le Song. Learning combinatorial optimization algorithms over graphs. In I. Guyon, U. V. Luxburg, S. Bengio, H. Wallach, R. Fergus, S. Vishwanathan, and R. Garnett, editors, *Advances in Neural Information Processing Systems*, volume 30. Curran Associates, Inc., 2017. URL <https://proceedings.neurips.cc/paper/2017/file/d9896106ca98d3d05b8cbdf4fd8b13a1-Paper.pdf>.
- [10] Ilias Diakonikolas, Vasilis Kontonis, Christos Tzamos, Ali Vakilian, and Nikos Zarifis. Learning online algorithms with distributional advice. In Marina Meila and Tong Zhang, editors, *Proceedings of the 38th International Conference on Machine Learning*, volume 139 of *Proceedings of Machine Learning Research*, pages 2687–2696. PMLR, 18–24 Jul 2021. URL <http://proceedings.mlr.press/v139/diakonikolas21a.html>.
- [11] John P. Dickerson, Karthik Abinav Sankararaman, Aravind Srinivasan, and Pan Xu. Assigning tasks to workers based on historical data: Online task assignment with two-sided arrivals. In *Proceedings of the 17th International Conference on Autonomous Agents and MultiAgent Systems, AAMAS ’18*, page 318–326, Richland, SC, 2018. International Foundation for Autonomous Agents and Multiagent Systems.
- [12] John P. Dickerson, Karthik Abinav Sankararaman, Aravind Srinivasan, and Pan Xu. Balancing relevance and diversity in online bipartite matching via submodularity. *Proceedings of the AAAI Conference on Artificial Intelligence*, 33(01):1877–1884, Jul. 2019. doi:10.1609/aaai.v33i01.33011877. URL <https://ojs.aaai.org/index.php/AAAI/article/view/4013>.
- [13] Paul Erdos and Alfred Renyi. On the evolution of random graphs. *Publ. Math. Inst. Hungary. Acad. Sci.*, 5:17–61, 1960.

-
- [14] Matthias Fey and Jan E. Lenssen. Fast graph representation learning with PyTorch Geometric. In *ICLR Workshop on Representation Learning on Graphs and Manifolds*, 2019.
 - [15] Justin Gilmer, Samuel S. Schoenholz, Patrick F. Riley, Oriol Vinyals, and George E. Dahl. Neural message passing for quantum chemistry. In *Proceedings of the 34th International Conference on Machine Learning - Volume 70*, ICML'17, page 1263–1272. JMLR.org, 2017.
 - [16] Gurobi Optimization, LLC. Gurobi Optimizer Reference Manual, 2021. URL <https://www.gurobi.com>.
 - [17] Aric A. Hagberg, Daniel A. Schult, and Pieter J. Swart. Exploring Network Structure, Dynamics, and Function using NetworkX. In Gaël Varoquaux, Travis Vaught, and Jarrod Millman, editors, *Proceedings of the 7th Python in Science Conference*, pages 11 – 15, Pasadena, CA USA, 2008.
 - [18] F. Maxwell Harper and Joseph A. Konstan. The movielens datasets: History and context. *ACM Trans. Interact. Intell. Syst.*, 5(4), December 2015. ISSN 2160-6455. doi:10.1145/2827872. URL <https://doi.org/10.1145/2827872>.
 - [19] Eric Jones, Travis Oliphant, Pearu Peterson, et al. SciPy: Open source scientific tools for Python, 2001–. URL <http://www.scipy.org/>.
 - [20] Chinmay Karande, Aranyak Mehta, and Pushkar Tripathi. Online bipartite matching with unknown distributions. In *Proceedings of the Forty-Third Annual ACM Symposium on Theory of Computing*, STOC '11, page 587–596, New York, NY, USA, 2011. Association for Computing Machinery. ISBN 9781450306911. doi:10.1145/1993636.1993715. URL <https://doi.org/10.1145/1993636.1993715>.
 - [21] Richard Karp, Umesh Vazirani, and Vijay Vazirani. An optimal algorithm for on-line bipartite matching. In *STOC '90*, 1990.
 - [22] Seyed Mehran Kazemi, Rishab Goel, Kshitij Jain, Ivan Kobyzev, Akshay Sethi, Peter Forsyth, and Pascal Poupart. Representation learning for dynamic graphs: A survey, 2020.
 - [23] Diederik P. Kingma and Jimmy Ba. Adam: A method for stochastic optimization. In Yoshua Bengio and Yann LeCun, editors, *3rd International Conference on Learning Representations, ICLR 2015, San Diego, CA, USA, May 7-9, 2015, Conference Track Proceedings*, 2015. URL <http://arxiv.org/abs/1412.6980>.
 - [24] Weiwei Kong, Christopher Liaw, Aranyak Mehta, and D. Sivakumar. A new dog learns old tricks: RL finds classic optimization algorithms. 2019. URL <https://openreview.net/pdf?id=rkluJ2R9KQ>.
 - [25] Wouter Kool, Herke van Hoof, and Max Welling. Attention, learn to solve routing problems! In *International Conference on Learning Representations*, 2019. URL <https://openreview.net/forum?id=ByxBFsRqYm>.
 - [26] Aranyak Mehta. Online matching and ad allocation. *Foundations and Trends in Theoretical Computer Science*, 8(4):265–368, 2013. URL <http://dx.doi.org/10.1561/04000000057>.
 - [27] Adam Paszke, Sam Gross, Francisco Massa, Adam Lerer, James Bradbury, Gregory Chanan, Trevor Killeen, Zeming Lin, Natalia Gimelshein, Luca Antiga, Alban Desmaison, Andreas Kopf, Edward Yang, Zachary DeVito, Martin Raison, Alykhan Tejani, Sasank Chilamkurthy, Benoit Steiner, Lu Fang, Junjie Bai, and Soumith Chintala. Pytorch: An imperative style, high-performance deep learning library. In H. Wallach, H. Larochelle, A. Beygelzimer, F. d'Alché-Buc, E. Fox, and R. Garnett, editors, *Advances in Neural Information Processing Systems 32*, pages 8024–8035. Curran Associates, Inc., 2019. URL <http://papers.neurips.cc/paper/9015-pytorch-an-imperative-style-high-performance-deep-learning-library.pdf>.
 - [28] Manish Purohit, Zoya Svitkina, and Ravi Kumar. Improving online algorithms via ml predictions. In S. Bengio, H. Wallach, H. Larochelle, K. Grauman, N. Cesa-Bianchi, and R. Garnett, editors, *Advances in Neural Information Processing Systems*, volume 31. Curran Associates, Inc., 2018. URL <https://proceedings.neurips.cc/paper/2018/file/73a427badebe0e32caa2e1fc7530b7f3-Paper.pdf>.
 - [29] Stephane Ross and Drew Bagnell. Efficient reductions for imitation learning. In Yee Whye Teh and Mike Titterton, editors, *Proceedings of the Thirteenth International Conference on Artificial Intelligence and Statistics*, volume 9 of *Proceedings of Machine Learning Research*, pages 661–668, Chia Laguna Resort, Sardinia, Italy, 13–15 May 2010. PMLR. URL <http://proceedings.mlr.press/v9/ross10a.html>.
 - [30] Richard S. Sutton and Andrew G. Barto. *Reinforcement Learning: An Introduction*. The MIT Press, second edition, 2018. URL <http://incompleteideas.net/book/the-book-2nd.html>.
 - [31] Hingfung Ting and Xiangzhong Xiang. Near optimal algorithms for online maximum weighted b-matching. In Jianer Chen, John E. Hopcroft, and Jianxin Wang, editors, *Frontiers in Algorithmics*, pages 240–251, Cham, 2014. Springer International Publishing. ISBN 978-3-319-08016-1.

-
- [32] Shufan Wang, Jian Li, and Shiqiang Wang. Online algorithms for multi-shop ski rental with machine learned advice. In H. Larochelle, M. Ranzato, R. Hadsell, M. F. Balcan, and H. Lin, editors, *Advances in Neural Information Processing Systems*, volume 33, pages 8150–8160. Curran Associates, Inc., 2020. URL <https://proceedings.neurips.cc/paper/2020/file/5cc4bb753030a3d804351b2dfec0d8b5-Paper.pdf>.
- [33] Yansheng Wang, Yongxin Tong, Cheng Long, Pan Xu, Ke Xu, and Weifeng Lv. Adaptive dynamic bipartite graph matching: A reinforcement learning approach. In *2019 IEEE 35th International Conference on Data Engineering (ICDE)*, pages 1478–1489, 2019. doi:10.1109/ICDE.2019.00133.

A Implementation Details

All environments are implemented in Pytorch [27]. We use Networkx [17] to generate synthetic graphs and find optimal solutions for E-OBM problems. Optimal solutions for OSBM problems are found using Gurobi [16] (See Appendix D). Pytorch Geometric [14] is used for handling graphs during training and implementing graph encoders. Our code is publicly available ².

B Training and Evaluation

B.1 Training Protocol

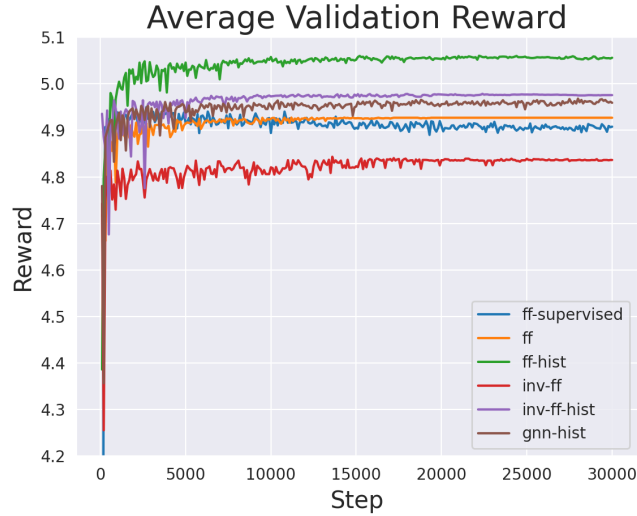


Figure 13: gMission 10x30. Note that `ff-supervised` starts at $\text{Reward} \approx 1.9$ at Epoch 0.

We train our models for 300 epochs on datasets of 20000 instances using the Adam optimizer [23]. We use a batch size of 200 except for MovieLens, where batch size 100 is used on graphs bigger than 10x60 due to memory constraints.

Training often takes less than 6 hours on a NVIDIA v100 GPU. `gnn-hist` takes less than a day to train on small graphs but consumes more time for bigger graphs and more complicated environments such as MovieLens 94x100. This is due to re-embedding the graph at every timestep which consumes more memory and computation as the graph size grows. We believe this can be improved with more efficient embedding schemes for dynamic graphs [22] but leave this for future work.

B.2 Node Features

Since `gnn-hist` supports node features by default, we leverage this property in order for incoming nodes to have "identities" that can be helpful to learn smarter strategies.

For the E-OBM problem, the ER and gMission datasets do not have any helpful node attributes that are not encoded in the edge weights. Therefore, we only provide node attributes that help the encoder differentiate between different types of nodes. That is, the skip node will get node feature -1 , any fixed node i will get feature (j_i) which is 1 if i is already matched and 0 otherwise, and incoming nodes have feature 2. These features simply help the model differentiate between incoming nodes, fixed nodes, and the node that represents the skipping action.

In the original MovieLens dataset, the incoming nodes are users while the fixed nodes are movies, both of which have helpful features. A fixed node i has feature vector (j_i, g_i) where g_i is a binary vector that represents the genres which the movie belongs to. The skip nodes will have feature vector $\vec{0}$. Incoming users have attributes

²<https://github.com/lyeskhali/CORL.git>

(gender, occupation, age), each of which is mapped to a number and normalized to between 0 and 1. See Table 4 for details.

Attribute	Categories	Feature Range
Gender	Male, Female	$0 \leq i \leq 1$
Age	<ul style="list-style-type: none"> • Under 18 • 18-24 • 25-34 • 35-44 • 45-49 • 50-55 • 56+ 	$0 \leq i \leq 6$
Occupation	<ul style="list-style-type: none"> • Other • academic/educator • artist • clerical/admin • college/grad student • customer service • doctor/health care • executive/managerial • farmer • homemaker • K-12 student • lawyer • programmer • retired • sales/marketing • scientist • self-employed • technician/engineer • tradesman/craftsman • unemployed • writer 	$0 \leq i \leq 20$

Table 4: User features in the MovieLens dataset.

B.3 Hyperparameter Tuning

Fixed Hyperparameters: The ff and ff-hist models have 3 hidden layers with 100 neurons each. inv-ff and inv-ff-hist have 2 hidden layers of size 100. gnn-hist model has 2 hidden layers of size 200 and used embedding dimension 30. All models use the ReLU non-linearity.

Hyperparameter	Range
Learning Rate	$\{j \times 10^{-i} 2 \leq i \leq 6, 1 \leq j \leq 9\}$
Learning Rate Decay	$\{1.0, 0.99, 0.98, 0.97, 0.96, 0.95\}$
Exponential Decay β	$\{1.0, 0.95, 0.9, 0.85, 0.8, 0.7, 0.65, 0.6\}$
Entropy Rate γ	$\{j \times 10^{-i} 1 \leq i \leq 4, 1 \leq j \leq 9\}$

Table 5: Hyperparameter Grid

Each RL model is tuned on 4 hyperparameters, as seen in Table 5, using a held-out validation set of size 1000. Figure 4 shows the top 200 hyperparameter search results for ff-hist. Each curve represents a hyperparameter configuration. Evidently, most configurations with small learning rates result in a high average optimality ratio. Other models also show similar results in being insensitive to minor hyperparameter changes.

B.4 Evaluation

greedy-rt baseline: As shown in Algorithm 1, greedy-rt works by randomly picking a threshold between 1 and $\lceil \ln(w_{max} + 1) \rceil$, where w_{max} is the maximum possible weight. When a new node comes in, we arbitrarily pick any

edge whose weight is at least the threshold, or skip if none exist. Surprisingly, this simple strategy is near optimal in the adversarial setting, with a competitive ratio of $\frac{1}{2e^{\lceil \ln(w_{max}+1) \rceil}}$.

Since `greedy-rt` does not support weights between 0 and 1, we re-normalize the edge weights in all E-OBM datasets. For ER and BA graphs, we multiply all weights by 100. For gMission graphs, we re-normalize by multiplying all weights by the maximum weight in the original dataset.

Algorithm 1 `greedy-rt`

```

1: Choose an integer  $K$  uniformly at random in the set  $N = \{1, 2, \dots, \lceil \ln(w_{max} + 1) \rceil\}$ 
2: Set  $\tau = e^K$ 
3: while a new vertex  $v \in V$  arrives do
4:    $A = \{u \mid u \text{ is } v\text{'s unmatched neighbor in } U \text{ and } w_{(u,v)} \geq \tau\}$ 
5:   if  $A = \emptyset$  then
6:     leave  $v$  unmatched
7:   else
8:     match  $v$  to an arbitrary vertex in  $A$ 

```

C Dataset Generation Details

C.1 Synthetic Graphs:

Erdos-Renyi (ER): We generate bipartite graph instances for the E-OBM problem using the Erdos-Renyi (ER) scheme [13]. Edge weights are sampled from the uniform distribution $U(0, 1]$. For each graph size e.g. 10x30, we generate datasets for a number of p values (the probability of edge creation).

Barabasi-Albert (BA): We follow the same process described by [5] for generating preferential attachment bigraphs. To generate a bigraph in this model, start with $|U|$ offline nodes and introduce online nodes V one at a time. The model has a single parameter p which is the average degree of an online node. Upon arrival of a new online node $v \in V$, we sample $n_v \sim \text{Binomial}(|U|, p/|U|)$ to decide the number of the neighbours of v . Let μ be a probability distribution over the nodes in U defined by $\mu(u) = \frac{1 + \text{degree}(u)}{|U| + \sum_{u \in U} \text{degree}(u)}$. We sample offline nodes from according to μ from U until n_v neighbours are selected.

C.2 Real-World Graphs:

gMission: In this setting, we have a set of workers available offline and incoming tasks which must be matched to compatible workers[8]. Every worker is associated with a euclidean location where the worker is present, the range within which it can serve tasks, and the success probability that it will complete any task. Tasks are represented by a euclidean location and a payoff value for being completed. We use the same strategy in [11] to pre-process the dataset. That is, workers that share similar locations are grouped into the same "type", and likewise for tasks. An edge is drawn between a worker and a task if the task is within the range of the worker. The edge weight is calculated by multiplying the payoff for completing the task with the success probability. In total, we have 532 worker types and 712 task types.

To generate a bipartite graph instance of size $|U|$ by $|V|$, we sample $|U|$ workers uniformly at random without replacement from the 532 types and sample $|V|$ tasks with replacement from \mathcal{D} . We set \mathcal{D} to be uniform. That is, the graph generation process involves sampling node from V in the base graph uniformly.

MovieLens: The dataset consists of a set of movies each belonging to some genres and a set of users which can arrive and leave the system at anytime. Once a user arrives, they must be matched to an available movie or left unmatched if no good movies are available. We have historical information about the average ratings each user has given for each genre. The goal is to recommend movies which are relevant and diverse genre-wise. This objective is measured using the weighted coverage function over the set of genres. Therefore, we must maximize the sum of the weighted coverage functions of all users which have arrived.

The MovieLens dataset contains a total of 3952 movies, 6040 users, and 100209 ratings of the movies by the users. As in [12], we choose 200 users who have given the most ratings and sample 100 movies at random. We, then, remove any movies which have no neighbors with the 200 users to get a total of 94 movies. These sets of movies and users will be used to generate all bipartite graphs. We calculate the average ratings each user has given for each genre. These average ratings will be used as the weights in the coverage function (See section 2.1). To generate an

instance of size $|U|$ by $|V|$, we sample $|U|$ movies uniformly at random without replacement from the 94 movies and $|V|$ users with replacement according to the uniform arrival distribution \mathcal{D} . The full graph generation procedure for gMission and MovieLens can be seen in Algorithm 2.

Algorithm 2 Graph Generation

```

1: procedure GENERATE( $K, T, \mathcal{D}, G(U^*, V^*, E^*), \text{type}, N$ )
2:    $D = \{\}$ 
3:   if type  $\neq$  "var" then ▷ if all graphs should have same fixed nodes
4:      $U = u_1, \dots, u_K \sim \text{Uniform}(U^*)$  ▷ Sample  $K$  fixed nodes without replacement from base graph
5:   while  $i < N$  do ▷ Generate  $N$  graphs
6:     if type = "var" then
7:        $U = u_1, \dots, u_K \sim \text{Uniform}(U^*)$  ▷ Re-sample for every graph
8:      $V, E = \{\}, \{\}$ 
9:     while  $j < T$  do ▷ Add  $T$  nodes to  $V$ 
10:       $v \sim \mathcal{D}(V^*)$  ▷ Sample according to arrival distribution  $\mathcal{D}$  from base graph
11:       $e = \{(u, v) : u \in U\}$ 
12:      if  $e = \phi$  then
13:        Go to Step 10 ▷ Re-sample if incoming node has no neighbors
14:       $V = V \cup \{v\}$ 
15:       $E = E \cup e$ 
16:       $j += 1$ 
17:       $D = D \cup \{G(U, V, E)\}$  ▷ Add graph instance to dataset
18:       $i += 1$ 
return  $D$  ▷ Return  $N$  graphs of size  $K$  by  $T$ 

```

D Finding Optimal Solutions Offline

To find the optimal solutions for E-OBM, we use the `linear_sum_assignment` function in the Scipy Library [19]. For OSBM (with the coverage function), we borrow the IP formulation from [12] defined below:

$$\begin{aligned}
& \text{Maximize} \quad \sum_{v \in V} \sum_{z \in [g]} w_{zv} \gamma_{zv} \\
& \text{Subject to} \quad \sum_{u \in \text{Ngr}(v)} x_{uv} \leq r_v, \forall v \in V \\
& \quad \sum_{v \in \text{Ngr}(u)} x_{uv} \leq 1, \forall u \in U \\
& \quad x_{uv} \in \{0, 1\} \\
& \quad \gamma_{zv} \leq \sum_{(u,v) \in E: q_{(u,v)}[z]=1} x_{(u,v)}, \forall z \in [g], v \in V \\
& \quad \gamma_{zv} \leq 1, \forall z \in [g], v \in V
\end{aligned}$$

Above, $[g]$ is the set of genres and z is used to index into each genre. Every edge is associated with a binary feature vector $q_{(u,v)}$ of dimension g .

E Permutation Invariance

In Figure 14, we show the results on gMission-perm where we train all models on the gMission dataset and test on the same dataset but with the fixed nodes permuted. We can see that the performance of the non-invariant models drops significantly compared to the gMission results in Figure 8. The invariant models are unaffected by the permutation as they receive *node-wise* input. `ff-hist` is less affected by this permutation in the 10x60 plot, this suggests that historical features help the model learn "identities" for each fixed node even if the nodes are permuted at test time. However, more incoming nodes need to be observed for the features to be statistically significant.

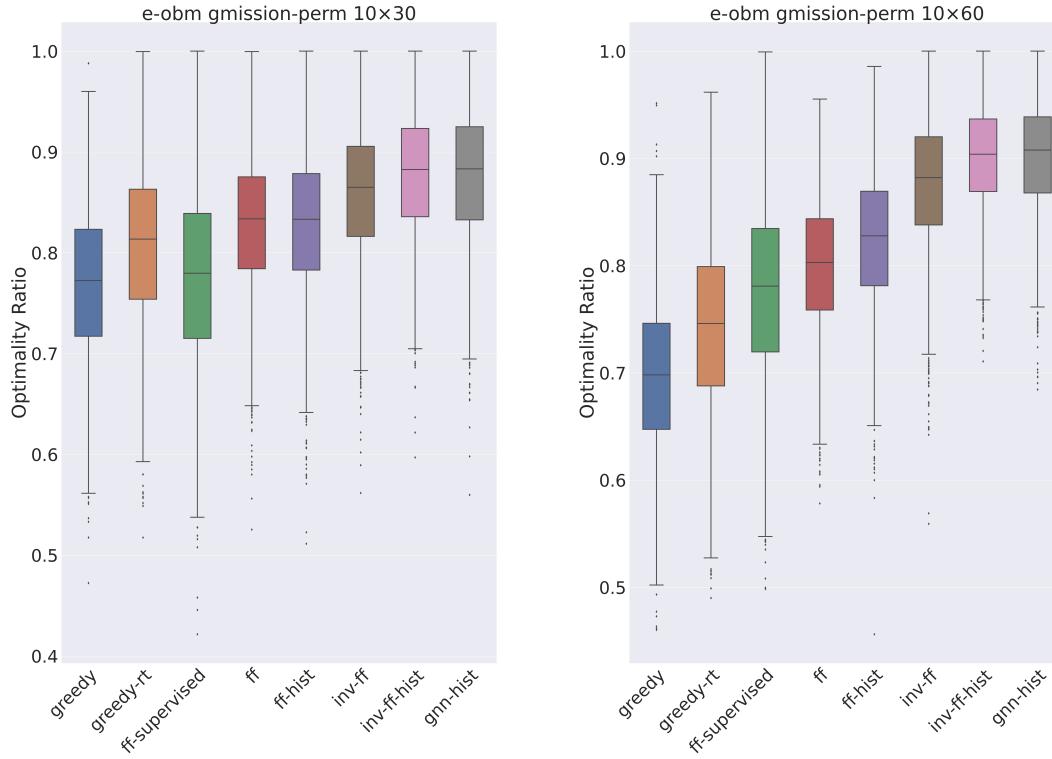


Figure 14: Distribution of Optimality Ratios for gMission-perm: gMission with Fixed Nodes Permuted at Test Time

F Agreement Plots

In Figure 16, greedy is closer to optimal for sparse graphs but gets increasingly different as the graphs get denser. This suggests that sparse graphs require a more greedy strategy as there not many options available in the future, while dense graphs with more incoming nodes than fixed nodes require a smarter strategy as the future may hold many better options.

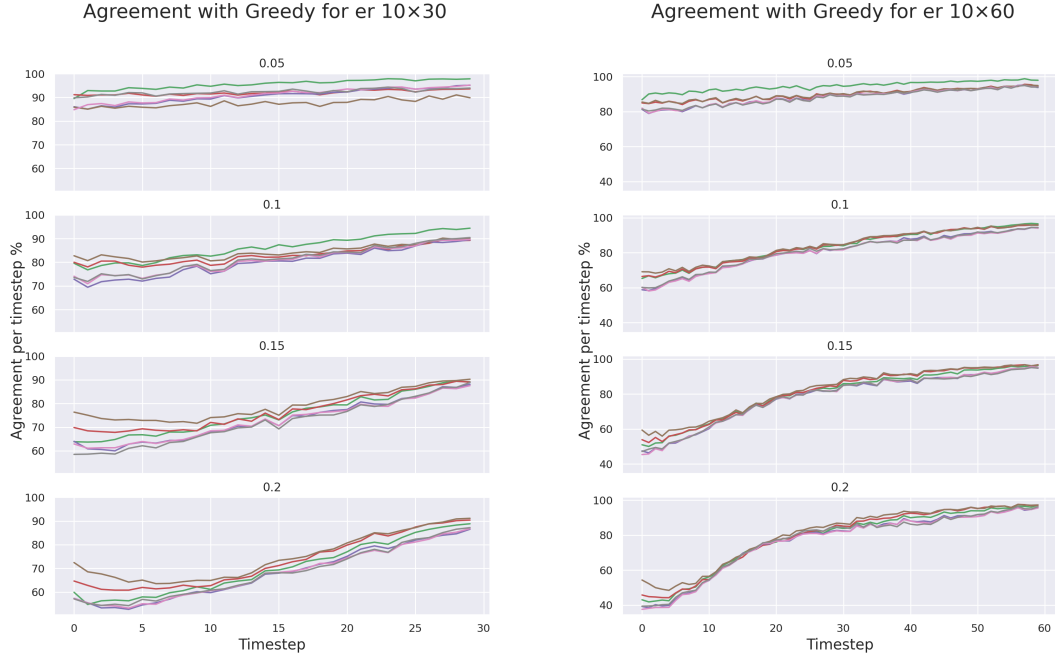


Figure 15: ER Agreement with Greedy Actions

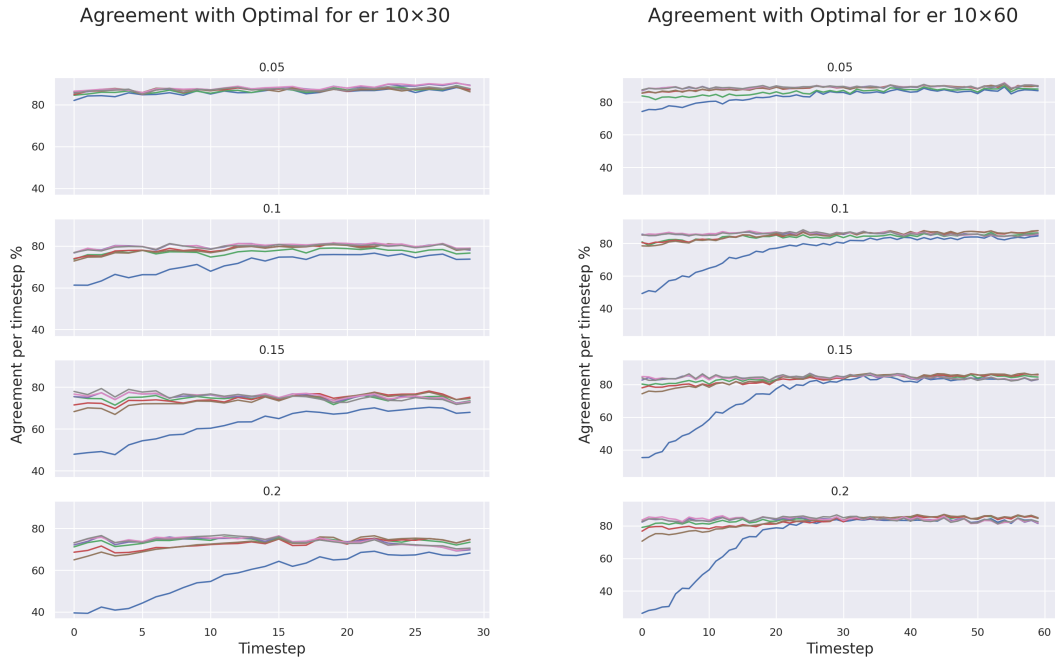


Figure 16: ER Agreement with Optimal Actions

For gMission 100x100, `inv-ff` learns to be almost exactly greedy. Other invariant models are closer to greedy in the beginning only. Non-invariant models learn very different strategies from greedy. Interestingly, while `ff-supervised` does not have the best performance on gMission 100x100, it is the closest to optimal in Figure 18. This is because the supervised model is learning to copy the optimal actions but lacks the sequential reasoning

that RL models possess. It is often the case that there are many different solutions besides opt that give high reward, so RL models may not necessarily learn the same strategy as **ff**-supervised.

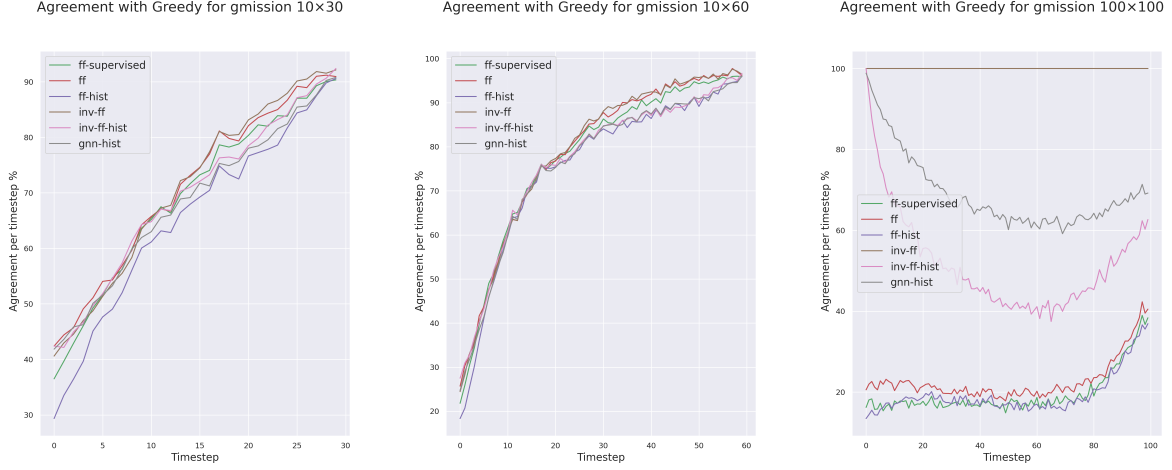


Figure 17: gMission Agreement with Greedy Actions

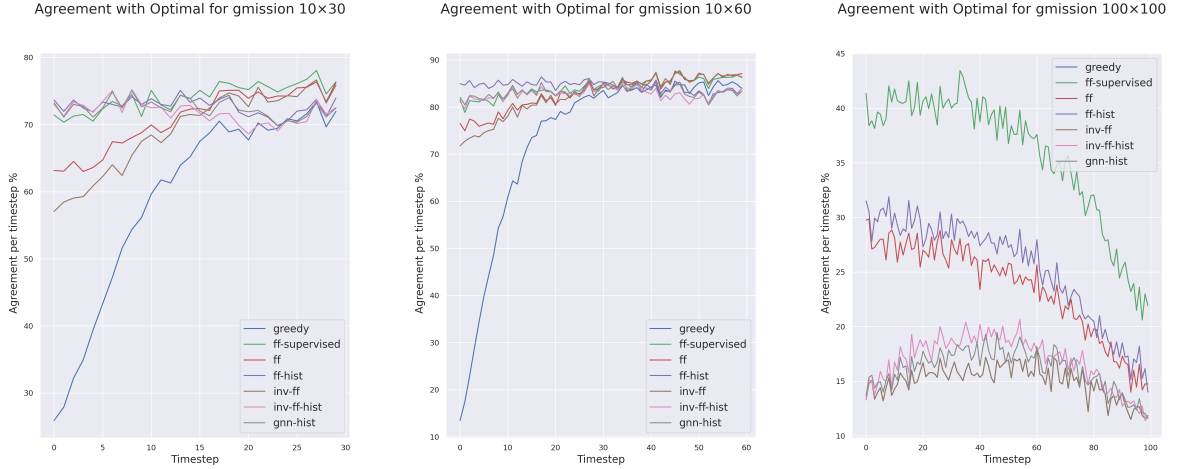


Figure 18: gMission Agreement with Optimal Actions

G Extension to other OBM Variants

All models and features were designed such that they can be applied to new OBM variants with little modifications. For example, to train our models on the Adwords problem, the input vector m (See Section 4.2) would instead be the remaining budget per advertiser. For the Display Ads problem, m would be the current capacity per advertiser. One could add problem specific features that give the models better context such as the average capacity or budget as well as initial budgets for each node in U . Models such as **gnn-hist** should ideally learn any useful problem-specific features without much modifications.